

Fibrin gel formation in a shear flow

ROBERT D. GUY^{a*}, AARON L. FOGELSON^{a,b†}, AND JAMES P. KEENER^{a,b‡}

Departments of Mathematics^a and Bioengineering^b

University of Utah

155 South 1400 East, Room 233

Salt Lake City, UT 84112-0090

[Received on 16 September 16 2005; revised on 2 May 2006]

Blood clots are made up of platelets and fibrin gel, and the relative amount of fibrin is strongly influenced by the shear rate. In order to explore this phenomenon, this paper presents a model of fibrin gel formation over the surface of an injured blood vessel in a shear flow. A condition for gelation including source and sink terms of polymer is derived. A simplified model of coagulation, involving activation and inhibition of the enzyme thrombin and thrombin-mediated production of fibrin monomer, is combined with the model of gelation to explore how the shear rate and other parameters control the formation of fibrin gel. The results show that the thrombin inhibition rate, the gel permeability, and the shear rate are key parameters in regulating the height of the fibrin gel.

Keywords: Blood Clotting, Blood Coagulation, Gelation, Smoluchowski Equation

1. Introduction

The formation of blood clots is essential for arresting bleeding and maintaining the integrity of the vascular system. Clots are the result of two interacting processes: platelet aggregation and coagulation. Injury to a blood vessel wall causes exposure to the blood of molecules embedded in the wall, including collagen and tissue factor. Blood platelets adhere to the collagen and become activated, thus beginning the process of platelet aggregation (Ruggeri 1994; Goto, Ikeda, Saldívar, and Ruggeri 1998). Tissue factor initiates the coagulation process which involves a tightly regulated network of enzyme reactions (Jesty and Nemerson 1995; Mann, Nesheim, Church, Haley, and Krishnaswamy 1990). The final product of these reactions is the enzyme thrombin, which is produced by reactions on the surfaces of activated platelets that convert the enzyme precursor prothrombin to the active enzyme thrombin. The thrombin is then released into the blood plasma where, among other things, it initiates fibrin polymerization (Weisel 2005; Mosesson 2005). It does this by converting the plasma protein fibrinogen into fibrin monomer. Thrombin cleaves short peptide fragments on the central domain of the fibrinogen molecule to expose a pair of binding sites. The newly exposed sites bind spontaneously to complimentary sites on the ends of other fibrin molecules. This linear polymerization yields protofibrils, which then laterally aggregate to form fibers. During lateral aggregation branch points form, and this process leads to the development of fibrin gel.

*Email: guy@math.utah.edu, corresponding author

†Email: fogelson@math.utah.edu

‡Email: keener@math.utah.edu

Fibrin polymerization has been studied intensely since the 1970s. Most fibrin experiments are done without flow, although all intravascular clots form in the presence of moving fluid. It has long been observed that fibrin-rich clots form under low shear rate conditions, but that under high-shear conditions, clots are predominantly made up of platelets (Frieman 1987; Weiss, Turitto, and Baumgartner 1986; Weiss, Baumgartner, and Turitto 1987). Consequently, venous clots have a preponderance of fibrin while the upstream portions of arterial clots are mainly platelets. Fibrin-rich extensions of these platelet-rich clots form on the downstream side of the platelet-rich clots where there is shelter from the rapidly moving flow. Exploring the mechanisms by which flow can modulate fibrin gel formation is a goal of this paper.

We have previously proposed models of the clotting process including a detailed treatment of the fluid mechanics during platelet aggregation (Fogelson and Guy 2004) and a comprehensive description of the biochemical reactions in coagulation with a simple treatment of flow-mediated transport (Kuharsky and Fogelson 2001; Fogelson and Tania 2005). The model developed and analyzed in this paper does not strive for a detailed description of the processes involved in fibrin-gel formation. It combines simple models of coagulation, gelation, and fluid-gel interaction in order to begin to understand how fibrin gel formation is influenced by the fluid motion. To our knowledge, the model presented in this paper is the first of chemically-induced gelation on a surface in a flowing environment.

In the remainder of this paper, we review an analysis of an existing model of gelation for the case that the total amount of polymers is fixed (Hendriks, Ernst, and Ziff 1983; Ziff and Stell 1980). If polymer is removed from this system, gelation may not occur (Hendriks 1984). We present an extension of the model to handle sources and sinks of polymer and derive a gelation condition that involves the relative rates of polymerization, polymer addition, and polymer removal. In Section 3 we present our model of fibrin formation in a shear flow over the surface of an injured blood vessel and describe how this model is combined with the gelation model to explore how the height of the gel depends on the model parameters. The results of the model are presented in Section 4, and finally in Section 5 we discuss the significance of the results and which aspects of the model will be expanded in future work.

2. Gelation

Gelation is the transition from polymers dissolved in solution to a gel. Roughly, one can think of a gel as a macroscopic network of polymer in solution that behaves as a solid. The early statistical theories of gelation of Flory (1941) and Stockmayer (1943) identified the onset of gelation as the weight-average molecular weight of polymers becoming unbounded. These early theories underlie percolation theory (Stauffer and Aharony 1992), which has been used to derive more detailed descriptions of the sol-gel transition (de Gennes 1976; Stauffer 1976; Stauffer, Coniglio, and Adam 1982). These models assume that bonds form randomly among some set of binding sites, and ignore the time evolution of the underlying kinetic processes.

Kinetic gelation models, which track the temporal evolution of polymers, are important for studying systems in which the gelation time and other properties of the system are strongly influenced by the sequence and rates of various reactions. Such methods are of two basic types. One is similar to random percolation models (Herrmann, Stauffer, and Landau 1983; Manneville and de Seze 1981) and uses stochastic simulations on a lattice to evaluate statistics of the evolving system. Another uses differential equations describing the concentrations of polymers of different sizes (Hendriks, Ernst, and Ziff 1983). We employ this second type of

model in this work because it is readily adapted to include source and sink terms of polymer and analytic methods can be used to predict gel formation. This type of modeling has been used for other aggregation processes in blood such as the formation of red cell rouleaux (Samsel and Perelson 1982; Samsel and Perelson 1984) and platelet-neutrophil aggregation (Laurenzi and Diamond 1999). In Section 2.1 we discuss gelation resulting from an initial distribution of polymers when there are no sources or sinks of polymers (Ziff and Stell 1980). There have been many reviews on models of coagulation and gelation, see for example Leyvraz (2003). The effect of removal terms on the gel time was studied by Singh and Rodgers (1996), and similarly, source terms were considered by Davies, King, and Wattis (1999). In Section 2.2 we derive a condition for gelation and compute the gel time including both source and sink terms of polymer.

2.1 Kinetic gelation model

Consider a spatially uniform mixture of polymers. Assume that each polymer is constructed from identical monomers each with n reaction groups (binding sites). Additionally assume $n \geq 3$, otherwise gelation is not possible. Let c_k represent the concentration of polymers constructed from k monomers (k -mers). Ignoring bond rupture, the evolution of the concentrations of k -mers is given by

$$\frac{dc_k}{dt} = \frac{1}{2} \sum_{i+j=k} K_{i,j} c_i c_j - \sum_m K_{m,k} c_m c_k, \quad (2.1)$$

where the coagulation kernel $K_{i,j}$ is the reaction rate between i -mers and j -mers. This equation is known as the Smoluchowski coagulation equation (Smoluchowski 1917).

The onset of gelation is marked by the blow up of the weight-average molecular weight of polymer, which is proportional to the second moment of the distribution of concentrations. The j^{th} moment is defined by

$$M_j = \sum_{\ell} \ell^j c_{\ell}. \quad (2.2)$$

The concentration of monomers that are in a k -mer is kc_k and the first moment M_1 is the total concentration of monomers. The probability, p_k , that any particular monomer is part of a k -mer is

$$p_k = \frac{kc_k}{M_1}. \quad (2.3)$$

Denote the weight of a monomer by m . Since all monomers are identical, the weight of a polymer constructed from k monomers is mk . The weight-average molecular weight of the clusters is

$$M_w = m \sum_k k p_k = m \frac{M_2}{M_1}. \quad (2.4)$$

If no gel is present and there are no sources or sinks of polymer, the total concentration of monomers (both free and in polymers) is conserved, making M_1 constant. Therefore the average weight is proportional to the second moment.

In the classical description of gelation, it is assumed that no rings or cycles can form within a polymer and that every unreacted binding site has an equal chance of reacting with an available site on another polymer. With these assumptions, the coagulation kernel is

$$K_{i,j} = k_g \left((n-2)i + 2 \right) \left((n-2)j + 2 \right), \quad (2.5)$$

where k_g is the rate of reaction between two binding sites. The expression $\left((n-2)i+2\right)$ is the number of available binding sites on an i -mer. Ziff and Stell (1980) used this kernel and expressed (2.1) as

$$\frac{dc_k}{dt} = \frac{k_g}{2} \sum_{i+j=k} \left((n-2)i+2\right) \left((n-2)j+2\right) c_i c_j - k_g \left((n-2)k+2\right) c_k R, \quad (2.6)$$

where R is the total number of reaction sites available. Expressing this last term in this form has the advantage that reaction sites in both the sol and gel can be included in R . In this paper we do not consider the solution beyond the gel point, so that

$$R = \sum_m \left((n-2)m+2\right) c_m. \quad (2.7)$$

To analyze the system (2.6), we introduce the generating function

$$g(z, t) = \sum_k z^{(n-2)k+2} c_k, \quad (2.8)$$

which satisfies the equation

$$\frac{\partial g}{\partial t} = k_g \frac{1}{2} \left(\frac{\partial g}{\partial z}\right)^2 - k_g z \frac{\partial g}{\partial z} R. \quad (2.9)$$

The moments of the distribution are related to the derivatives of this generating function at $z = 1$ and the individual concentrations are related to the derivatives at $z = 0$.

Detecting gelation does not require solving (2.9), as we only need to determine when the second moment becomes unbounded. The first three moments are related to the derivatives of g at $z = 1$ by

$$M_0(t) = g(1, t) \quad (2.10)$$

$$R(t) = g_z(1, t) = (n-2)M_1 + 2M_0 \quad (2.11)$$

$$W(t) = g_{zz}(1, t) = (n-2)^2 M_2 + 3(n-2)M_1 + 2M_0. \quad (2.12)$$

Evolution equations for these three quantities are found by differentiating equation (2.9) with respect to z and setting $z = 1$. The resulting equations are

$$\frac{dM_0}{dt} = -\frac{k_g}{2} R^2 \quad (2.13)$$

$$\frac{dR}{dt} = -k_g R^2 \quad (2.14)$$

$$\frac{dW}{dt} = k_g (W^2 - 2RW) \quad (2.15)$$

Define a new variable $Y = W - R$, which satisfies

$$\frac{dY}{dt} = k_g Y^2. \quad (2.16)$$

The value of Y is related to the moments by

$$Y = (n-2)^2 M_2 + 2(n-2)M_1. \quad (2.17)$$

When gelation occurs Y must become unbounded, and conversely the blow-up of Y indicates gelation because M_1 is constant. The solution to (2.16) is

$$Y = \frac{Y(0)}{1 - Y(0)k_g t}, \quad (2.18)$$

which becomes unbounded at time

$$t_g = \frac{1}{Y(0)k_g}. \quad (2.19)$$

This time marks the appearance of gel.

2.2 Gelation with a source and sink

In the previous section, we discussed gelation for a given distribution of polymers that begin reacting at the initial time. In our model of fibrin formation, monomers are constantly being produced because of the interaction of thrombin and fibrinogen. Polymers are also being removed as the moving fluid transports them away from the injury site. In this section we include source and sink terms in the equation for the polymers, and we derive conditions for gelation for the case of a constant source and sink.

To the equations for the distribution of polymers, we include source and sink terms. With these modifications, equation (2.6) becomes

$$\frac{dc_k}{dt} = \frac{k_g}{2} \sum_{i+j=k} \left((n-2)i+2 \right) \left((n-2)j+2 \right) c_i c_j - k_g \left((n-2)k+2 \right) c_k R + S_k - \beta c_k, \quad (2.20)$$

where S_k is the source of k -mers and β is the rate of removal. The removal rate is taken to be a constant, independent of polymer size. In the model of fibrin formation presented in Section 3, the removal is by transport by flow, which depends on the fluid velocity and not the polymer size. The equation for the generating function defined by (2.8) is

$$\frac{\partial g}{\partial t} = k_g \frac{1}{2} \left(\frac{\partial g}{\partial z} \right)^2 - k_g z \frac{\partial g}{\partial z} R + P(z) - \beta g, \quad (2.21)$$

where

$$P(z) = \sum_k S_k z^{(n-2)k+2}. \quad (2.22)$$

As in the previous section, we use the variable $Y = g_{zz}(1, t) - g_z(1, t)$ to detect gelation. The equation for Y with the source and sink terms is

$$\frac{dY}{dt} = k_g Y^2 + \Pi - \beta Y, \quad (2.23)$$

where

$$\Pi = P''(1) - P'(1). \quad (2.24)$$

The behavior of the solution to (2.23) depends on whether the polynomial

$$k_g \lambda^2 - \beta \lambda + II = 0 \quad (2.25)$$

has real or complex roots.

First consider the case when

$$\beta^2 - 4k_g II > 0, \quad (2.26)$$

so that both roots of (2.25) are positive and real. Let λ_- denote the smaller root and λ_+ denote the larger root. The solution to (2.23) is

$$Y(t) = \frac{\lambda_- - \lambda_+ \alpha \exp(-\kappa t)}{1 - \alpha \exp(-\kappa t)}, \quad (2.27)$$

where

$$\kappa = (\beta^2 - 4k_g II)^{1/2} \quad \text{and} \quad \alpha = \frac{Y(0) - \lambda_-}{Y(0) - \lambda_+}. \quad (2.28)$$

Gelation may or may not occur, depending on the initial condition. If $\alpha < 1$, $Y(t)$ remains finite for all time, but if $\alpha > 1$, gelation occurs at time

$$t_g = \kappa^{-1} \ln(\alpha). \quad (2.29)$$

In terms of the initial condition for Y , gelation occurs if and only if $Y(0) > \lambda_+$. In the model of fibrin formation, the relevant initial condition is $Y(0) = 0$, which means that fibrin gel cannot form if (2.26) holds.

Suppose instead that

$$\beta^2 - 4k_g II < 0, \quad (2.30)$$

so that the roots of (2.25) are complex. The solution of (2.23) is

$$Y(t) = \frac{\beta + a \tan\left(at/2 + \arctan\left((2k_g Y(0) - \beta)/a\right)\right)}{2k_g}, \quad (2.31)$$

where

$$a = (4k_g II - \beta^2)^{1/2}. \quad (2.32)$$

In this case gel forms for any initial condition, and the gel time is

$$t_g = \left(\pi - 2 \arctan\left((2k_g Y(0) - \beta)/a\right)\right)/a. \quad (2.33)$$

Thus we have shown that for initial conditions of no polymer, gelation occurs if and only if $\beta^2 < 4k_g II$. An interpretation of this result is that gelation can be prevented by removing polymers from the system faster than they can form gel. In the model of fibrin gel formation detailed in the next section, (2.30) is used to indicate if fibrin gel can form.

3. Model of fibrin formation

In this section we present a model of fibrin formation in a shear flow over an injured blood vessel surface. We assume that platelets attached to this surface produce thrombin. Concentrations of enzymes and proteins vary with vertical distance from the injury, but we assume that their concentrations are constant along the length of the injury, giving a one-dimensional model. We refer to this domain as the injury zone and consider the concentrations outside it as given. Fibrinogen and prothrombin are carried into the injury zone from upstream at a rate proportional to the fluid velocity. Prothrombin is converted to thrombin at the surface of the injured vessel, and thrombin is degraded by antithrombin III. Thrombin converts fibrinogen to fibrin monomer, which then polymerizes to produce larger polymers and possibly fibrin gel. Besides the prothrombin to thrombin conversion, all reactions take place throughout the domain. A schematic of the reactions is depicted in Figure 1. All reactants, except gel, are removed from the injury zone at a rate proportional to the fluid velocity.

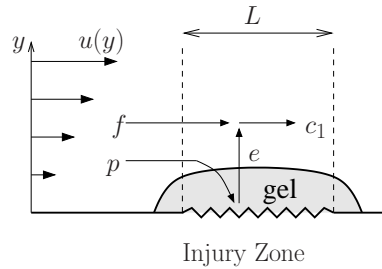


FIG. 1. Schematic of reactions in the model of fibrin gel formation over an injured blood vessel surface. Prothrombin, p , and fibrinogen, f , are transported into the injury zone by the fluid. Prothrombin is converted to thrombin, e , at the injured surface ($y = 0$). Thrombin converts fibrinogen to fibrin monomer, c_1 , which then polymerizes. All concentrations are removed from the injury zone at a rate proportional to the fluid velocity, $u(y)$.

3.1 Model Equations

The equations for the concentrations of prothrombin (p) and thrombin (e) in the injury zone are

$$\frac{\partial p}{\partial t} = D \frac{\partial^2 p}{\partial y^2} - \frac{u}{L} (p - p_{\text{up}}) \quad (3.1)$$

$$\frac{\partial e}{\partial t} = D \frac{\partial^2 e}{\partial y^2} - \frac{u}{L} e - k_{\text{at}} e, \quad (3.2)$$

where D is the diffusion coefficient, L is the length of the injury zone, k_{at} is the degradation rate of thrombin, u is the fluid velocity, and p_{up} is the upstream concentration of prothrombin. These two equations are coupled by the boundary condition at the injured surface ($y = 0$) where prothrombin is converted into thrombin. We take the boundary conditions at $y = 0$ to

be

$$\frac{\partial p}{\partial y} = \frac{k_{\max}}{k_s + p} p \quad (3.3)$$

$$\frac{\partial e}{\partial y} = -\frac{k_{\max}}{k_s + p} p. \quad (3.4)$$

In Appendix A, we relate the rate constants to physical quantities. Boundary conditions for other variables are discussed in the next section.

The equation for the fibrinogen concentration (f) is similar to the prothrombin equation, except that it contains a reaction term corresponding to the conversion of fibrinogen to fibrin;

$$\frac{\partial f}{\partial t} = D_f \frac{\partial^2 f}{\partial y^2} - \frac{u}{L} (f - f_{\text{up}}) - \frac{k_f e}{k_{fs} + f} f. \quad (3.5)$$

Because the conversion of fibrinogen to fibrin monomer is enzymatic, this reaction term is taken to be of Michaelis-Menten type. For fibrin we use equations of the form (2.20) to keep track of the concentrations of the sizes of polymerizing fibrin. Only the equation for the monomers contains a source term, and the removal rate depends on the fluid velocity. The equations for the polymer concentrations are

$$\frac{dc_k}{dt} = \frac{k_g}{2} \sum_{i+j=k} \left((n-2)i + 2 \right) \left((n-2)j + 2 \right) c_i c_j - k_g c_k R + \delta_{1k} \frac{k_f e}{k_{fs} + f} f - \frac{u}{L} c_k, \quad (3.6)$$

where δ is the Kronecker delta. We assume that the diffusion of fibrin polymer is negligible for all sizes of fibrin polymer. This assumption allows us to use the results from section 2.2 for gelation with a source and sink. In reality the diffusion of polymer should be a decreasing function of polymer size, but it is reasonable to ignore diffusion because the time scales of advection and polymerization reactions are expected to be substantially faster.

This model is not used to solve for the concentrations of polymers, rather we only seek to determine if gelation is possible using the condition derived in the previous section. Because only monomers contribute to the source term, the form of Π from (2.22) and (2.24) is

$$\Pi = n(n-2) \frac{k_f e}{k_{fs} + f} f. \quad (3.7)$$

Recall that n represents the number of binding sites on each monomer. This description of polymerization is not intended to capture the full complexity of fibrin polymerization and gelation. As a tractable model of chemically-induced gelation in flow, it is used to gain insight into blood clotting without accounting for the details of the fibrin reactions.

To complete the formulation of the model, we must describe how the fluid velocity profile is computed. In the absence of gel, the velocity profile is linear because it is a shear flow. In the gel layer, we use the Brinkmann equation (Stokes equation with an added drag term) to account for the friction between the fluid and the stationary porous gel (Ethier and Kamm 1989; Weinbaum, Zhang, Han, Vink, and Cowin 2003). The equation for the velocity profile is

$$\mu \frac{\partial^2 u}{\partial y^2} - \xi u = 0, \quad (3.8)$$

where μ is the fluid viscosity and ξ is the hydraulic resistivity (drag coefficient) that depends on the permeability of the gel.

3.2 Steady-state Model of Gel Height

The model described in the previous section is used to assess how the different parameters and the shear rate interact to limit the growth of gel. We seek to determine whether the gel reaches a certain height such that further gelation cannot occur at the surface, thus limiting the growth of gel. In Section 2.2 we derived a condition for gelation given constant source and removal rates. For the model of fibrin gel formation, the removal rate is

$$\frac{u}{L}, \quad (3.9)$$

and the source term consists of only monomers with strength

$$\frac{k_f e f}{k_{fs} + f}. \quad (3.10)$$

The condition for gelation in terms of the fibrin model from (2.30) is

$$\frac{u}{L} < \sqrt{4k_g n(n-2)} \frac{k_f e f}{k_{fs} + f}. \quad (3.11)$$

We define the maximum gel height h to be the height of the gel such that (3.11) holds for $y < h$ and fails to hold for $y \geq h$ when all the concentrations are in steady state. Below we argue that such a height exists and discuss the algorithm used to find it.

At the injured surface ($y = 0$) the velocity is zero, making the left side of (3.11) zero. This means that for any nonzero thrombin and fibrinogen concentration gel is always able to form near the injured surface. As the gel surface gets farther from the injured surface, the concentration of thrombin at the gel surface decreases towards zero. Because the concentration of fibrinogen is bounded by the upstream concentration, the source strength decreases to zero as the gel height increases. We show below that the velocity at the surface is an increasing function of the gel height. Therefore it must be that at some height (3.11) fails, and a maximum gel height exists.

To compute the maximum gel height, we solve equation (3.8) with a given gel height and hydraulic resistivity (ξ) to obtain the velocity field. We then solve for the concentration profiles of prothrombin, thrombin, and fibrinogen at steady-state to compute the rate of fibrin monomer production. With the velocity and monomer source strength computed at the gel surface, we use the (3.11) to determine if gelation is possible at the surface of the gel. Beginning with zero gel height, we repeat the above computation increasing the gel height incrementally until gelation is impossible at the surface. At this height the right and left sides of (3.11) are equal. For each set of parameters, we vary the shear rate and use the above procedure to see how the maximum gel height depends on the shear rate.

To complete the formulation of the model, we must describe how the velocity profile of the fluid is computed. This requires a model for how the hydraulic resistivity, ξ , depends on the gel permeability. For simplicity, we assume that the hydraulic resistivity is a positive constant where there is gel and zero where there is no gel. Thus the hydraulic resistivity is a piecewise constant function in space. A more detailed model of how the gel feeds back on the fluid is beyond the scope of this work and is discussed further in Section 5. When the concentrations of prothrombin, thrombin, and fibrinogen are taken in steady state, there is a constant source

of fibrin monomer. Within an existing gel, this constant production of fibrin yields a constant increase in gel mass. However, even as more gel is produced, with ξ given as described above, the velocity profile of the fluid remains unchanged. Thus the existence of a steady state solution results from this simple model for the hydraulic resistivity.

At the injured surface, $y = 0$, the velocity is zero, and far away from the gel surface the velocity profile is assumed to be that of a linear shear flow with the given shear rate γ . With these boundary conditions, the velocity profile is

$$u = \begin{cases} \gamma \ell_o \frac{\sinh(y/\ell_o)}{\cosh(h/\ell_o)} & y < h \\ \gamma(y - h + \ell_o \tanh(h/\ell_o)) & y \geq h \end{cases}, \quad (3.12)$$

where h is the height of the gel, and

$$\ell_o = \left(\frac{\mu}{\xi} \right)^{1/2}. \quad (3.13)$$

The parameter ℓ_o represents the characteristic length scale of the decay of the velocity profile within the gel. We call this parameter the penetration depth, and it is one of the parameters we vary in exploring the model's behavior.

Finally, we describe the boundary conditions for fibrinogen, prothrombin, and thrombin. At the top boundary, we impose Dirichlet conditions of the upstream conditions. In the computations, the top boundary is always sufficiently far from the surface of the gel so as not to influence the results. The boundary condition for fibrinogen at the injured surface is a no flux condition. In Appendix A we discuss the boundary conditions for prothrombin and thrombin at the injured surface ($y = 0$). As is argued there, and numerical computations confirm, the maximum gel height is insensitive to surface reaction rates and all of these are taken to be 1 s^{-1} for all of the computations. In summary, the boundary conditions at the injured surface ($y = 0$) are

$$\frac{\partial p}{\partial y} = \frac{k_{\max}}{k_s + p} p \quad (3.14)$$

$$\frac{\partial e}{\partial y} = -\frac{k_{\max}}{k_s + p} p \quad (3.15)$$

$$\frac{\partial f}{\partial y} = 0 \quad (3.16)$$

$$u = 0, \quad (3.17)$$

and at $y = \infty$ the boundary conditions are

$$p = p_{\text{up}} \quad (3.18)$$

$$e = 0 \quad (3.19)$$

$$f = f_{\text{up}} \quad (3.20)$$

$$\frac{\partial u}{\partial y} = \gamma, \quad (3.21)$$

where p_{up} and f_{up} are the plasma concentrations of prothrombin and fibrinogen, respectively.

3.3 Parameters and Scalings

The equations for prothrombin, thrombin, and fibrinogen are nondimensionalized before solving them. The prothrombin and thrombin concentrations are scaled by the upstream concentration of prothrombin, p_{up} . Similarly, fibrinogen and fibrin are scaled by the upstream concentration of fibrinogen, f_{up} . Lengths are scaled by the length of the injury zone, L , which we set to $100 \mu\text{m}$ for computations. The diffusion coefficient for fibrinogen is about $2 \cdot 10^{-7} \text{ cm}^2/\text{s}$ (Larsson, Blomback, and Rigler 1987; Bark, Földes-Papp, and Rigler 1999), and the diffusion coefficient for prothrombin/thrombin is about $4 \cdot 10^{-7} \text{ cm}^2/\text{s}$ (Hubbell and McIntire 1986). For simplicity, we take the diffusion coefficient to be $10^{-7} \text{ cm}^2/\text{s}$ for enzymes as well as for fibrinogen.

In the equations for prothrombin and thrombin, (3.1) and (3.2) respectively, the only parameter to explore is the rate of thrombin inhibition, k_{at} . In the fibrinogen equation (3.5), there are two additional parameters in the reaction term, k_f and k_{fs} . We do not vary these parameters directly, rather, we consider the combinations

$$\kappa_f = \frac{k_f p_{\text{up}}}{f_{\text{up}}}, \quad (3.22)$$

and

$$\kappa_{fs} = \frac{k_{fs}}{f_{\text{up}}}. \quad (3.23)$$

The parameter κ_f is a scaled rate of reaction with units s^{-1} , and κ_{fs} is the nondimensional saturation constant. Similarly, rather than prescribe k_g , we vary

$$\kappa_g = k_g f_{\text{up}}, \quad (3.24)$$

which appears in the gelation condition. Finally we take the number of binding sites, n , that appears in (3.11), to be three. This choice is somewhat arbitrary, and it only affects the effective polymerization rate.

We now estimate values for the penetration depth (ℓ_0), thrombin inhibition rate (k_{at}), polymerization rate (κ_g), fibrin production rate (κ_f), and the saturation constant (κ_{fs}). These parameter estimates are used as starting values for explorations, and in the next section we explore the effects of modifying each of these parameter values.

The value of the penetration depth for fibrin is estimated to be on the order of $1 \mu\text{m}$ (Wootton, Popel, and Alevriadou 2002). This value depends on the microstructure of the gel, which depends on the conditions under which the gel is formed (Ryan, Mockros, Weisel, and Lorand 1999). Considering the microstructure of the gel is beyond the scope of this work, and so we begin with $\ell_o = 2 \mu\text{m}$ as a starting value. We note that the hydraulic resistivity of fibrin is much lower (and ℓ_o much larger) than other physiological fibrous materials (Levick 1987).

Estimates of the rate at which thrombin is degraded by antithrombin III vary from 0.02 s^{-1} (Hubbell and McIntire 1986) to 0.2 s^{-1} (Kuharsky and Fogelson 2001). We begin with $k_{\text{at}} = 0.1 \text{ s}^{-1}$ as a base value of the inhibition rate. This value is chosen from the high side of the range of estimates to account for the possibility of other inhibition mechanisms of the coagulation network, which are not directly modeled in this work.

Typical plasma concentrations of prothrombin and fibrinogen are around $1 \mu\text{M}$ and $10 \mu\text{M}$, respectively. The reaction rate of fibrin monomer binding (Aa binding) has been measured or estimated in the range $6 \cdot 10^5 \text{ M}^{-1}\text{s}^{-1}$ to $1 \cdot 10^6 \text{ M}^{-1}\text{s}^{-1}$ (Hantgan and Hermans 1979; Lewis,

Shields, and Shafer 1985; Weisel, Veklich, and Gorkun 1993). Using this as an approximation for k_g , we estimate $\kappa_g = 10 \text{ s}^{-1}$ as a reasonable polymerization rate for fibrin. For the conversion of fibrinogen to fibrin, Higgins, Lewis, and Shafer (1983) report $k_f = 84 \text{ s}^{-1}$ and $k_{fs} = 7.2 \text{ }\mu\text{M}$, and other studies report similar values (Vindigni and Di Cera 1996). We use $\kappa_f = 10 \text{ s}^{-1}$ and $\kappa_{fs} = 1$ for the fibrin production rate and saturation constant, respectively.

4. Results

For a given set of parameters, we compute the maximum gel height for shear rates in the physiologically relevant range of 50 s^{-1} and 1500 s^{-1} . A typical plot of the maximum gel height vs. shear rate is shown in Figure 2. As expected, the maximum gel height decreases as the shear rate increases, but the rate of decrease is much greater for low shear rates, and there is a transition to a different behavior for high shear rates. This raises the questions of what determines where the transition between low and high shear rates occurs and what factors limit the gel growth in these two regimes.

In Figure 3 the maximum gel height as a function of shear rate is plotted for three different penetration depths. The shape of the curves is the same: they are identical at high shear rates and at low shear rates the maximum gel height decreases at the same rate. This plot shows that the permeability of the gel determines the range of shear rates at which the transition occurs between these behaviors.

When the shear rate is low and the gel height is much larger than the penetration depth ($h \gg \ell_o$) the velocity at the gel surface is

$$u_h = \gamma \ell_o \tanh\left(\frac{h}{\ell_o}\right) \approx \gamma \ell_o, \quad (4.1)$$

which is independent of the gel height and proportional to the penetration depth. For a given low shear rate, the velocity at the gel surface is lower when ℓ_o is lower, and so the maximum gel height is higher. This is reflected by the results in Figure 3 at low shear. On the other hand, when the shear rate is high and the gel height is smaller than the penetration depth ($h < \ell_o$), the velocity at the gel surface is

$$u_h = \gamma \ell_o \tanh\left(\frac{h}{\ell_o}\right) \approx \gamma h, \quad (4.2)$$

which is independent of the penetration depth and depends on the height. This explains why the curves in Figure 3 overlap at high shear rates. Because the velocity at the surface is sensitive to different variables at low and high shear rates, a transition in behavior occurs when the maximum gel height is on the order of the penetration depth. For larger penetration depths this transition occurs at lower shear rates for two reasons: the maximum gel height is lower and the height where the transition occurs is larger.

As noted above, when the gel height is much greater than the penetration depth, the velocity at the gel surface is essentially independent of the gel height. In this regime, the removal rate of reactants is insensitive to the gel height, and something other than the removal rate limits the gel growth. As we discuss below, the availability of thrombin at the surface limits the gel height at low shear rates.

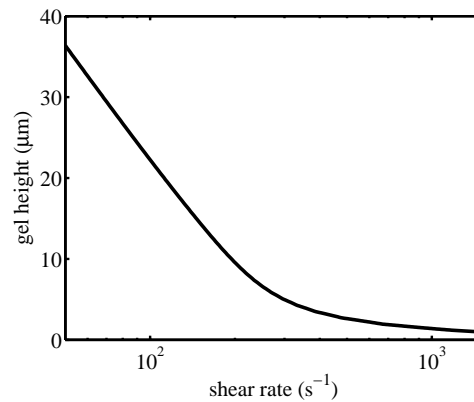


FIG. 2. Plot of typical result for the maximum gel height as a function of the shear rate. The parameters are $\ell_o = 2 \mu\text{m}$, $k_{\text{at}} = 0.1 \text{ s}^{-1}$, $\kappa_{\text{g}} = 10 \text{ s}^{-1}$, $\kappa_{\text{f}} = 10 \text{ s}^{-1}$, $\kappa_{\text{fs}} = 1$.

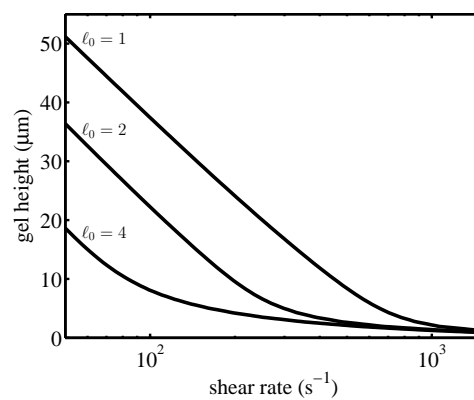


FIG. 3. Maximum gel height as a function of shear rate for three different penetration depths (gel permeabilities). The other parameters are $k_{\text{at}} = 0.1 \text{ s}^{-1}$, $\kappa_{\text{g}} = 10 \text{ s}^{-1}$, $\kappa_{\text{f}} = 10 \text{ s}^{-1}$, $\kappa_{\text{fs}} = 1$.

Figure 4 shows how the maximum gel height changes in response to changing the thrombin inhibition rate. For all inhibition rates, the maximum gel height is the same at high shear rates. However, at low shear rates the behavior of the gel is very different for the different inhibition rates. When the gel is thick, the fluid velocity within the gel is essentially zero through most of the gel layer. Thrombin produced at the injured surface must travel by diffusion to the gel surface. As the height of the surface increases, the time it takes for thrombin to reach the gel surface increases. For large inhibition rates thrombin is degraded rapidly and for the same shear rate the maximum gel height must be lower.

So far we have discussed how the gel permeability, the thrombin inhibition rate, and the shear rate combine to control gel height. We now discuss the effects of other parameters, namely the fibrin polymerization rate (κ_g), the thrombin/fibrinogen reaction rate (κ_f), and its saturation constant (κ_{fs}). Figure 5 shows how the polymerization rate affects the maximum gel height. It is not surprising that as the polymerization rate increases, the maximum gel height increases. The effect of changing this rate does not alter the basic behavior of the gel height as a function of the shear rate.

Next we consider the parameters related to the conversion of fibrinogen to fibrin. When the saturation constant is small ($\kappa_{fs} \ll 1$), the rate of fibrin production is independent of the fibrinogen concentration, and when the saturation constant is large ($\kappa_{fs} \gg 1$), the rate of fibrin production is linear in the fibrinogen concentration. That is,

$$\frac{\kappa_f e}{\kappa_{fs} + f} f \approx \begin{cases} \kappa_f e & \text{if } \kappa_{fs} \ll 1 \\ \frac{\kappa_f}{\kappa_{fs}} e f & \text{if } \kappa_{fs} \gg 1 \end{cases} . \quad (4.3)$$

In Figure 6(a), the maximum gel height is plotted against the shear rate for three different saturation constants and reaction rates. The saturation constant for case (i) is such that the fibrin source rate is independent of the fibrinogen concentration. Case (ii) has the same value of κ_f as in case (i) but the saturation constant is 1 so that the nonlinearity of the reaction rate is relevant. The saturation constant in case (iii) is such that the reaction rate is in the linear regime. The value of κ_f in case (iii) is chosen so that κ_f/κ_{fs} has the same value as κ_f in cases (i) and (ii). As this plot shows, the maximum gel height is not very sensitive to these parameters. To see why this is the case, in Figure 6(b), we plot the fibrinogen concentration profile for these three different parameter sets at shear rate 200 s^{-1} ; the markers on the curves denote the height of the gel surface. In these three cases, the amount of fibrinogen within the gel may be different, but the concentrations at the gel surface are similar.

5. Discussion

The goal of this paper is to explore what is responsible for limiting fibrin gel growth in different flow regimes. To our knowledge, the model presented in this paper is the first to examine the interplay between coagulation, gelation, and flow in limiting the growth of fibrin gel. Each of these processes is extremely complex, and so to begin to understand the interaction between them we have combined simple models of the individual parts.

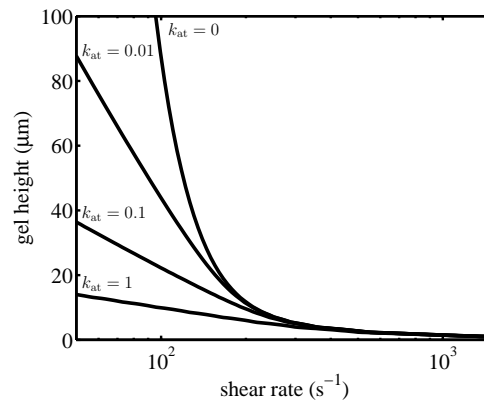


FIG. 4. Plot comparing the the maximum gel height for different thrombin inhibition rates. The other parameters are $\ell_o = 2 \mu\text{m}$, $\kappa_g = 10 \text{ s}^{-1}$, $\kappa_f = 10 \text{ s}^{-1}$, $\kappa_{fs} = 1$.

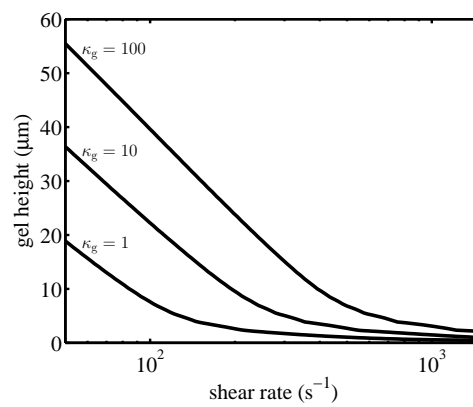


FIG. 5. Plot showing how the fibrin polymerization rate affects the maximum gel height. The other parameters are $\ell_o = 2 \mu\text{m}$, $k_{\text{at}} = 0.1 \text{ s}^{-1}$, $\kappa_f = 10 \text{ s}^{-1}$, $\kappa_{fs} = 1$

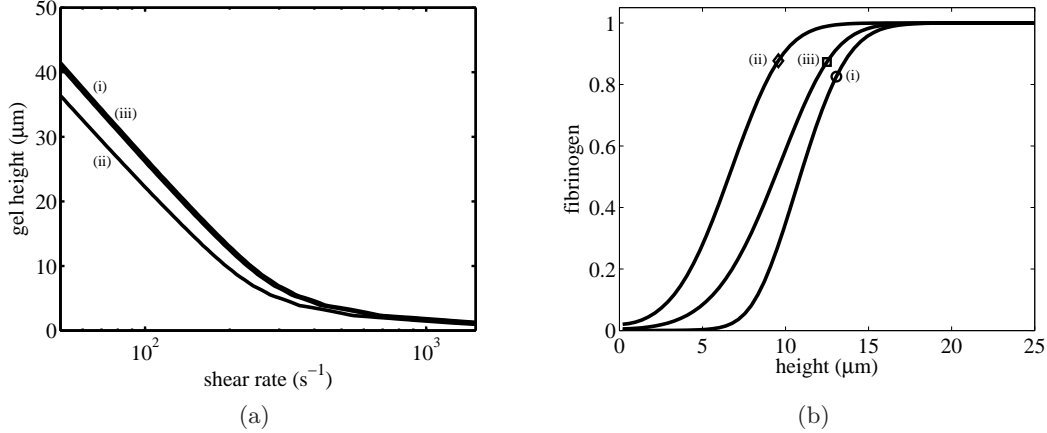


FIG. 6. Each plot contains curves for the three sets of fibrinogen reaction parameters. These parameters are (i) $\kappa_f = 10$, $\kappa_{fs} = 0.1$; (ii) $\kappa_f = 10$, $\kappa_{fs} = 1$; (iii) $\kappa_f = 100$, $\kappa_{fs} = 10$. The other parameters are $\ell_o = 2 \mu\text{m}$, $k_{\text{at}} = 0.1 \text{ s}^{-1}$, $\kappa_g = 10 \text{ s}^{-1}$. (a) Maximum gel height as a function of shear rate. (b) Concentration profiles of fibrinogen at shear rate $\gamma = 200 \text{ s}^{-1}$. The markers denote the height of the gel.

When monomers begin polymerizing, they do not instantaneously form gel. Gelation is indicated by the blow-up of the second moment of the distribution of polymer sizes. Using a kinetic model of polymerization, we derived expressions for the gel time by solving for a quantity related to the second moment. For initial conditions of no polymer, this analysis gave a condition for gelation involving the polymerization rate, removal rate, and source strength.

The gelation condition was combined with a reduced model of coagulation, which included thrombin activation on an injured surface, thrombin inhibition, and the conversion of fibrinogen to fibrin in the fluid. The concentrations of reactants and the fluid velocity vary with distance from the injured surface. For a given gel height we computed the concentrations of enzymes and proteins and the velocity profile at steady state, and then used the gelation condition to determine if the gel could continue to grow. At some point the gel reaches a height beyond which further gelation is impossible. We call this height the maximum gel height. To determine what factors influence this maximum gel height in different flow regimes, we plotted the maximum gel height against the shear rate for different sets of model parameters.

The results show that at low shear rates the availability of thrombin limits gel growth. At high shear rates, polymers are removed from the injury zone by the fluid motion before gelation occurs, thus limiting the gel growth. The transition from the low shear behavior to the high shear behavior is determined by the gel permeability. The polymerization rate and the reaction rate between thrombin and fibrinogen affected the maximum gel height, but these parameters did not alter the qualitative response of the gel height to changes in the shear rate. The results from this model give valuable insight into how the processes of flow, coagulation and gelation interact to limit fibrin gel growth. The results also indicate which aspects of the model deserve a more detailed treatment in future modeling.

Because the gel permeability played such an important role in controlling gel height, the model of this quantity should be examined further. In the model of this paper, the permeability was assumed to be homogeneous throughout the gel layer. Extending the model to include the

evolution of the gel density and structure is nontrivial. In this paper, we were only concerned with whether gelation was possible, which could be determined from analytic solutions for the moments of the distribution of polymer sizes. In the time dependent case, analytic solutions are not available because the source and sink terms of polymer change in time and depend on the evolution of many other quantities. Additionally, to determine the rate of gel production, one must solve for the generating function numerically, up to and *beyond* the gel point. Great care must be taken because of the singular nature of the problem. We are currently working on a time dependent version of the model.

In addition to including time dependent gel growth, natural directions for expansion of the model are multiple spatial dimensions and a more detailed description of coagulation. Real clots do not grow in one dimension, and the interactions between the evolving clot geometry and flow are expected to be much more complex. The model results predict that the availability of thrombin is particularly important at low shear rates in controlling clot size. The only mechanisms in the model to limit thrombin are inhibition by antithrombin III and removal by the flow. Other mechanisms, including chemical inhibition of other parts of the coagulation system and limitation on transport through a clot because of platelet aggregation (Kuharsky and Fogelson 2001; Hathcock and Nemerson 2004) may limit the production of thrombin. These effects could be included with a more detailed model of the coagulation reactions.

Acknowledgments

This work was supported in part by NSF FRG grant #DMS-0139926.

References

- Bark, N., Z. Földes-Papp, and R. Rigler (1999). The incipient stage in thrombin-induced fibrin polymerization detected by FCS at the single molecule level. *Biochem Biophys Res Commun* 260, 35–41.
- Davies, S. C., J. R. King, and J. A. D. Wattis (1999). The Smoluchowski coagulation equations with continuous injection. *J Phys A: Math Gen* 32, 7745–7763.
- de Gennes, P. G. (1976). On a relation between percolation theory and the elasticity of gels. *J Phys Lett* 37, L1.
- Ethier, C. and R. Kamm (1989). Flow through partially gel-filled channels. *Physicochemical Hydrodynamics* 11, 219–227.
- Flory, P. J. (1941). Molecular size distribution in three dimensional polymers. I. Gelation. *J Am Chem Soc* 63, 3083–3090.
- Fogelson, A. L. and R. D. Guy (2004). Platelet-wall interactions in continuum models of platelet aggregation: Formulation and numerical solution. *Mathematical Biology and Medicine* 21, 293–334.
- Fogelson, A. L. and N. Tania (2005). Coagulation under flow: The influence of flow-mediated transport on the initiation and inhibition of coagulation. *Pathophysiology of Haemostasis and Thrombosis* 34, 91–108.
- Frieman, D. (1987). The structure of thrombi. In R. W. Colman, J. Hirsh, V. J. Marder, and E. W. Salzman (Eds.), *Hemostasis and Thrombosis: Basic Principles and Clinical*

- Practice*, pp. 1123–1135. Philadelphia: J.B. Lippincott Company.
- Goto, S., Y. Ikeda, E. Saldívar, and Z. M. Ruggeri (1998). Distinct mechanisms of platelet aggregation as a consequence of different shearing flow conditions. *J Clin Invest* 101(2), 479–486.
- Hantgan, R. R. and J. Hermans (1979). Assembly of fibrin: A light scattering study. *J Biol Chem* 254, 11272–11281.
- Hathcock, J. J. and Y. Nemerson (2004). Platelet deposition inhibits tissue factor activity: In vitro clots are impermeable to Factor Xa. *Blood* 104(1), 123–127.
- Hendriks, E. M. (1984). Exact solution of a coagulation equation with removal term. *J Phys A: Math Gen* 17, 2299–2303.
- Hendriks, E. M., M. H. Ernst, and R. M. Ziff (1983). Coagulation equations with gelation. *J Stat Phys* 31, 519–563.
- Herrmann, H. J., D. Stauffer, and D. P. Landau (1983). Computer simulation of a model for irreversible gelation. *J Phys A: Math Gen* 16, 1221–1239.
- Higgins, D. L., S. D. Lewis, and J. A. Shafer (1983). Steady state kinetic parameters for the thrombin-catalyzed conversion of human fibrinogen to fibrin. *J Biol Chem* 258, 9276–9282.
- Hubbell, J. A. and L. V. McIntire (1986). Platelet active concentration profiles near growing thrombi: A mathematical consideration. *Biophys J* 50, 937–945.
- Jesty, J. and Y. Nemerson (1995). The pathways of blood coagulation. In E. Beutler, M. Lichtman, and B. Coller (Eds.), *Williams Hematology* (5th ed.), pp. 1227–1238. New York: McGraw-Hill.
- Kuharsky, A. L. and A. L. Fogelson (2001). Surface-mediated control of blood coagulation: The role of binding site densities and platelet deposition. *Biophys J* 80(3), 1050–1074.
- Larsson, U., B. Blomback, and R. Rigler (1987). Fibrinogen and the early stages of polymerization to fibrin as studied by dynamic laser light scattering. *Biochim Biophys Acta* 915, 172–179.
- Laurenzi, I. J. and S. L. Diamond (1999). Monte carlo simulation of the heterotypic aggregation kinetics of platelets and neutrophils. *Biophys J* 77, 1733–1746.
- Levick, J. R. (1987). Flow through interstitium and other fibrous matrices. *Q J Exp Physiol* 72, 409–438.
- Lewis, S. D., P. P. Shields, and J. A. Shafer (1985). Characterization of the kinetic pathway for liberation of fibrinopeptides during assembly of fibrin. *J Biol Chem* 260, 10192–10199.
- Leyvraz, F. (2003). Scaling theory and exactly solved models in the kinetics of irreversible aggregation. *Phys Rep* 383, 95–221.
- Mann, K. G., M. E. Nesheim, W. R. Church, P. Haley, and S. Krishnaswamy (1990). Surface-dependent reactions of the vitamin K-dependent enzyme complexes. *Blood* 76, 1–16.
- Manneville, P. and L. de Seze (1981). Percolation and gelation by additive polymerization. In J. Della Dora, J. Demongeot, and B. Lacolle (Eds.), *Numerical Methods in the Study of Critical Phenomena*. Berlin: Springer.

- Mosesson, M. (2005). Fibrinogen and fibrin structure and function. *Journal of Haemostasis and Thrombosis* 3, 1894–1904.
- Ruggeri, Z. M. (1994). New insights into the mechanisms of platelet adhesion and aggregation. *Semin Hematol* 31, 229–39.
- Ryan, E. A., L. F. Mockros, J. W. Weisel, and L. Lorand (1999). Structural origins of fibrin clot rheology. *Biophys J* 77, 2813–2826.
- Samsel, R. W. and A. S. Perelson (1982). Kinetics of rouleau formation. I. A mass action approach with geometric features. *Biophys J* 37, 493–514.
- Samsel, R. W. and A. S. Perelson (1984). Kinetics of rouleau formation. II. Reversible reactions. *Biophys J* 45, 805–824.
- Singh, P. and G. J. Rodgers (1996). Coagulation processes with mass loss. *J Phys A: Math Gen* 29, 437–450.
- Smoluchowski, M. V. (1917). Versuch einer mathematischen theorie der koagulation kinetic kolloider losungen. *Z Phys Chem* 92, 129–168.
- Stauffer, D. (1976). Gelation in concentrated critically branched polymer solutions. Percolation scaling theory of intramolecular bond cycles. *J Chem Soc Faraday Trans II* 72, 1354–1364.
- Stauffer, D. and A. Aharony (1992). *Introduction to Percolation Theory* (2nd ed.). London: Taylor and Francis.
- Stauffer, D., A. Coniglio, and M. Adam (1982). Gelation and critical phenomena. *Adv Polym Sci* 44, 103–158.
- Stockmayer, W. H. (1943). Theory of molecular size distribution and gel formation in branched-chain polymers. *J Chem Phys* 11, 45–55.
- Vindigni, A. and E. Di Cera (1996). Release of fibrinopeptides by the slow and fast forms of thrombin. *Biochemistry* 35, 4417–4426.
- Weinbaum, S., X. Zhang, Y. Han, H. Vink, and S. C. Cowin (2003). Mechanotransduction and flow across the endothelial glycocalyx. *Proc Nat Acad Sci* 100, 7988–7995.
- Weisel, J. W. (2005). Fibrinogen and fibrin. *Adv Protein Chem* 70, 247–299.
- Weisel, J. W., Y. Veklich, and O. Gorkun (1993). The sequence of cleavage of fibrinopeptides from fibrinogen is important for protofibril formation and enhancement of lateral aggregation. *J Mol Biol* 232, 285–297.
- Weiss, H. J., H. R. Baumgartner, and V. T. Turitto (1987). Regulation of platelet-fibrin thrombi on subendothelium. *Ann NY Acad Sci* 516, 380–97.
- Weiss, H. J., V. T. Turitto, and H. R. Baumgartner (1986). Role of shear rate and platelets in promoting fibrin formation on rabbit subendothelium. studies utilizing patients with quantitative and qualitative platelet defects. *J Clin Invest* 78, 1072–1082.
- Wootton, D. M., A. S. Popel, and R. Alevriadou (2002). An experimental and theoretical study on the dissolution of mural fibrin clots by tissue-type plasminogen activator. *Biotechnol Bioeng* 77, 405–419.
- Ziff, R. M. and G. Stell (1980). Kinetics of polymer gelation. *J Chem Phys* 73, 3492–3499.

A. Boundary Conditions for Prothrombin/Thrombin

In this section we describe the boundary conditions for prothrombin and thrombin in more detail. We first give expressions for the constants k_{\max} and k_s in terms of other parameters, and then discuss why the maximum gel height is insensitive to the values of the various reaction rates at the surface.

A.1 Surface Reactions

Prothrombin near the injured surface may bind to an available binding site on the surface of an activated platelet. The bound prothrombin is converted to thrombin, which then unbinds from the surface. Let p_s and e_s denote the concentrations of bound prothrombin and thrombin, respectively. These concentrations satisfy the equations

$$\frac{dp_s}{dt} = k_b b p - k_r p_s \quad (\text{A.1})$$

$$\frac{de_s}{dt} = k_r p_s - k_u e_s, \quad (\text{A.2})$$

where k_b is the rate of binding to the surface, b is the concentration of available binding sites, $p = p(0, t)$ is the fluid-borne concentration of prothrombin at the boundary, k_r is the rate of conversion of prothrombin to thrombin, and k_u is the unbinding rate. The rates of binding and unbinding to the surface appear in the boundary conditions for the fluid-borne concentrations as

$$-D \frac{\partial p}{\partial y} = -k_b b p \quad (\text{A.3})$$

$$-D \frac{\partial e}{\partial y} = k_u e_s. \quad (\text{A.4})$$

Assuming that the surface reactions are fast, equations (A.1) and (A.2) are taken in steady state. This allows us to solve for p_s and e_s and eliminate them in the boundary conditions for p and e . Note that the diffusive fluxes of prothrombin and thrombin are equal and opposite when the surface reactions are in steady state.

The number of available binding sites depends on the concentration of bound sites. Suppose that the total number of sites is fixed, so that $b = b^T - p_s - e_s$. Equations (A.1) and (A.2) at steady state are

$$k_b (b^T - p_s - e_s) p - k_r p_s = 0 \quad (\text{A.5})$$

$$k_r p_s - k_u e_s = 0, \quad (\text{A.6})$$

Solving this system for e_s ,

$$e_s = \frac{k_r k_b p}{k_r k_u + k_b (k_r + k_u) p} \quad (\text{A.7})$$

By defining the constants

$$k_s = \frac{k_r k_u}{k_b (k_r + k_u)} \quad (\text{A.8})$$

$$k_{\max} = \frac{k_b b^T}{D} k_s, \quad (\text{A.9})$$

the boundary conditions for prothrombin and thrombin, (A.3) and (A.4), are

$$\frac{\partial p}{\partial y} = \frac{k_{\max}}{k_s + p} p \quad (\text{A.10})$$

$$\frac{\partial e}{\partial y} = -\frac{k_{\max}}{k_s + p} p. \quad (\text{A.11})$$

A.2 Sensitivity

In exploring the model's behavior, we observed in computational tests that the gel height was insensitive to the surface reaction rates for reasonable choices of rates. In this section we discuss why this is the case. When the system is nondimensionalized, the prothrombin (and thrombin) concentration is scaled by its upstream concentration p_{up} and length is scaled by the length of the injury zone, L . With these scalings, the dimensionless constant in place of k_{\max} is

$$\kappa_{\max} = \frac{k_{\max} L}{p_{\text{up}}} = \frac{k_r k_u b^T L}{D p_{\text{up}} (k_r + k_u)}. \quad (\text{A.12})$$

This expression can be rearranged as

$$\kappa_{\max} = \left(1 + \frac{k_r}{k_u}\right)^{-1} \left(\frac{b^T}{L p_{\text{up}}}\right) \left(\frac{k_r L^2}{D}\right). \quad (\text{A.13})$$

We expect the first term in this product to be order one, as the unbinding rate is likely at least as fast as the reaction rate. The second term is the ratio of the concentration of surface binding sites to a surface concentration of prothrombin. The third term in the product is the ratio of the diffusion time scale to the reaction time. Estimating $D = 10^{-7} \text{ cm}^2/\text{s}$ and $L = 100 \text{ }\mu\text{m}$, the diffusion time scale is 10^3 s . We expect the reaction time to be significantly faster than this diffusion time. As long as the second term in the above expression for κ_{\max} is not abnormally small, we may assume that $\kappa_{\max} \gg 1$.

Because κ_{\max} is large, the other reaction rates (k_r, k_b, k_u) do not affect the computation of the gel height significantly. Consider the model problem

$$\frac{\partial^2 p}{\partial y^2} = 0 \quad (\text{A.14})$$

$$\frac{\partial p}{\partial y} = \frac{\kappa_{\max} p}{k_s + p}; \quad y = 0 \quad (\text{A.15})$$

$$p = p_0; \quad y = h \quad (\text{A.16})$$

For $\kappa_{\max} \gg 1$, the derivative at $y = 0$ is

$$\frac{\partial p}{\partial y} = \frac{p_0}{h} + \mathcal{O}(\kappa_{\max}^{-1}). \quad (\text{A.17})$$

This explains why in our exploratory computations, the gel height was insensitive to the parameters related to the reactions at the surface.